

Original Research

A Data-Based Reliability Analysis of ESP Failures in Oil Production Wells

Shaikha Al-Ballam ¹, Hamidreza Karami ^{2,*}, Deepak Devegowda ²1. Kuwait Oil Company, Ahmadi, Kuwait; E-Mail: shaikha.alballam@ou.edu2. Norman, Oklahoma, United States; E-Mails: karami@ou.edu; deepak.devegowda@ou.edu* **Correspondence:** Hamidreza Karami; E-Mail: karami@ou.edu**Academic Editor:** Francesco Gabriele Galizia**Special Issue:** [Energy Efficiency in Flexible and Reconfigurable Manufacturing: Emerging Trends, Models and Applications in the Industry 4.0 Era](#)*Journal of Energy and Power Technology*
2022, volume 4, issue 4
doi:10.21926/jept.2204036**Received:** September 27, 2022**Accepted:** November 02, 2022**Published:** November 14, 2022

Abstract

Electrical Submersible Pumps (ESPs) are one of the most widely used artificial lift methods in the petroleum industry. However, ESP failures are unanticipated and common occurrences with significant financial impacts for the operators. Analysis of the ESP performance and failures are essential in its design and optimization. This paper presents a statistical approach for diagnosing and evaluating the root causes of ESP failures. The analysis is based on the field data gathered from the surface and downhole ESP monitoring equipment over five years of production of 10 wells. Electrical failures are the most common general cause of ESP failures, accounting for 61% of all failures, followed by motor failure and gas locking. Specifically, power failure, under-voltage, voltage unbalance, and motor underload are the most common occurrences. The data trends are analyzed for the two weeks before each specific failure, and conclusions are made on the warning signs to predict failures. In addition, a Weibull statistical analysis model is constructed to evaluate the reliability features and estimate the ESP failure probability, allowing operators to perform preventive maintenance. The results provide guidelines for ESP operations and contribute to reducing or preventing ESP downtimes and operating costs.



© 2022 by the author. This is an open access article distributed under the conditions of the [Creative Commons by Attribution License](#), which permits unrestricted use, distribution, and reproduction in any medium or format, provided the original work is correctly cited.

Keywords

ESP statistical analysis; ESP reliability analysis; field data; ESP failures; case studies

1. Introduction

With the ever-declining production rates from oil and gas fields worldwide, the demand for efficient artificial lift techniques to enhance production is increasing daily [1]. The selection of a suitable artificial lift technique for a given well is a function of various operational parameters [2]. However, the goal is always to maximize the profit from the well by increasing production while maintaining the artificial lift-related expenses and downtime to a minimum. This is what makes a thorough understanding of the operating ranges, limitations, and failures of an artificial lift technique vital before its application.

Electrical Submersible Pumps (ESPs) are one of the most widely used artificial lift techniques in the petroleum industry, especially for highly productive oil wells [3]. They can provide noticeable increases in a well's production if looked after and maintained within their optimum operating range. However, ESP failures are usually sudden and unanticipated in the oil field and could become common occurrences. These failures cause significant financial impacts for the operators due to oil production deferrals and high intervention costs [4]. In addition, excessive shutdowns and trips significantly reduce the run-life of an ESP [5].

Production monitoring and surveillance of ESP wells help extend their run life. Furthermore, an ESP monitoring system is highly beneficial for recording a pump's performance and acquiring valuable data on the downhole conditions. These data are used to analyze and predict failures before they occur. These data involve various operations and field conditions, including dynamic, static, and historical data. They are the key factors for data-driven models predicting ESP system failures [6].

Mohrbacher and Tabe discussed ESP installation, operation, maintenance, and issues, including a system failure analysis [7, 8]. From the 1990s through 2010, several authors used statistical models to examine ESP problems. There were comparisons of failure distributions among the system components [9], different equipment types and models [10], or different companies, platforms, and fields [11]. In addition, historical trends have been used to assess the evolution of ESP run life through time. Past studies [10-12] presented statistical distributions fitted to historical data to forecast future failure frequencies. Sawaryn *et al.* emphasized the need to include all the ESP system parts in the study [13]. They suggested that the simulation time be extended to encompass the whole life of a field and appropriately measure ESP reliability. Furthermore, Alhanati *et al.* provided a standardized ESP failure analysis that included a list of all ESP-related failure types, failed items, failure descriptors, and root causes [14].

The failure rates of ESPs across an oilfield have been demonstrated to vary significantly [15]. Given the large number of ESPs installed in each oilfield, ESP failure prediction research mainly concentrates on computing population-level estimations and failure causes [16]. Sawaryn developed analytic terms to describe failure patterns at a population level [17]. Liu *et al.* also modified the data mining classification techniques [18].

1.1 Evolution of ESP Monitoring System Over Time

The monitoring levels of ESP systems have changed over time. The first and most straightforward method of diagnosing an ESP system’s failure is using ammeter charts to measure and record the current drawn by the downhole motor [4]. The wellhead pressure is then utilized to calculate the pump's head in the wellbore, followed by fluid shots to measure the fluid level. Fluid shots are useful but may be inaccurate owing to factors like foamy crude or completion configuration [19]. Recently, it has been possible to safeguard an ESP by forcing a pump shutdown depending on underload and overload current values, which is a sign of poor operating conditions.

The variable speed drive (VSD) was the next stage in the growth of ESP technology. This equipment gives operators an extra means of controlling an ESP’s functions while protecting pumps and motors from electrical stress. The main advantage of a VSD is that it allows the operator to modify the ESP's speed in response to variations in the well's productivity index or changing well conditions [20].

The introduction of the ESP Downhole Monitoring System was the next significant step in the evolution of ESP monitoring and control. This system gathers and transmits data from the downhole system to the surface, where it may be recorded and researched to optimize system performance and longevity. These devices have helped to improve the accuracy of the most crucial production metrics. They are becoming more prevalent, with a growing number of new installations equipped with them [5].

The ESP Downhole Monitoring System analyses well characteristics and delivers pump data to improve ESP efficiency and reserve recovery rates [21]. It helps to keep track of key operational parameters, as indicated in Table 1.

Table 1 Main Parameters Recorded in an ESP Downhole Monitoring System [21, 22].

Parameter	To determine:
Pump Intake Pressure (PIP), psi	Static and flowing bottom hole pressures
Pump Intake Temperature (Ti), °F	Gas Volume Fraction at the pump intake
Pump Discharge Pressure (Pd), psi	Head and efficiency of the pump
Pump Discharge Temp (Td), °F	Optional
Motor Temperature (Tm), °F	Operating temperature rise (Tm – Ti)
Current Leakage (mA)	Indication of impending ground fault conditions
Vibration (Vx & Vy)	Bearing mechanical wear and frequency that causes excessive vibration (Resonance).
Motor Frequency, Hz	Motor speed
Motor Current (I), Amps	Changes in fluid density and power consumption

The aforementioned parameters indicate the most relevant aspects to consider when analyzing ESP failures [23-25]. Even though appropriate monitoring helps delay system failures, they may still happen for various reasons [19]. Because the electrical system is typically the weakest link in an ESP system, most failures are electrical, resulting from a mechanical problem as the underlying cause of

the failure [26]. Each failure must be thoroughly probed, and its fundamental reason must be determined. Mubarak *et al.* [27] researched ESP failures in the Wafra field over four years and discovered that the most common causes of ESP failures include motor failures (40%), pump failures (22%), cable failure (26%), and others (12%). Furthermore, according to Al-Sadah [28], the most common reasons for ESP failures based on the Dismantle, Inspection, and Failure Analysis (DIFA) results are burnt motor (28%), damaged cable/MLE (27%), and damaged penetrator (24%). This study uses a comprehensive set of data from multiple oil wells with ESP systems to further analyze the ESP failures over time and explain the root physical causes.

The following sections detail the evaluation of statistical failure data, case studies of ESP failures, and an overview of ESP-specific failures. This overview highlights the reported ESP-specific failure modes and their corresponding early warning indicators in the ESP parameters, which may be used as a general guideline to detect ESP operating difficulties more efficiently and with less effort. The discussion then shifts to ESP reliability analysis, where correct assessment and forecasting of ESP failure probability led to a greater understanding of system performance. Finally, the conclusion outlines the most significant findings from the study.

2. Statistical Analysis Approach

This study presents a detailed analysis based on actual field data from Kuwait Oil Company (KOC) assets. For the evaluation, these data are categorized into static, dynamic, and historical data from over five years of production of 10 active wells. The dynamic high-frequency data was obtained from surface and downhole ESP monitoring equipment (VSD, pump, and wellhead). The static data includes the current well completion, ESP pump design, and reservoir fluid information. The dataset incorporates the failure's cause, the downtime's duration, and the corresponding pump data. Furthermore, historical operational data is used to supplement the analysis.

In our study, each well is equipped with gas separators to separate the free gas from the producing fluid before entering the pump. In addition, the ESP pump motors used in our study are typically two-pole, three-phase induction motors with squirrel cages. The motors operate at a nominal speed of 3500 rpm at 60 Hz or 2915 rpm at 50 Hz with a two-pole configuration. They run on three-phase power between 230 and 5,000 volts and between 12 and 200 amps. The diameter and length of the motors determine their horsepower ratings, and since there are no wires running along their lengths, the motors may be built somewhat larger than the pumps.

2.1 ESP Statistical Failure Data Evaluation

A statistical evaluation of the observed ESP failures in the available field data of this study is investigated in depth. The findings of our analysis are depicted in Figure 1, dividing the failures into a few main categories. In addition, Figure 2 shows a more specific division of the most statistically important causes for ESP failures. The evaluation includes 971 ESP failures from over 5 years of production from 10 wells. The detailed Specific Failures are shown in Table S1, Table S2, Table S3, and Table S4. Some of the most witnessed general failure roots are:

- Electrical Failure (61%): includes power fail, under/over voltage, phase unbalance, and overcurrent.
- Motor Failure (18%): includes motor voltage unbalance, motor overload, overheating, etc.

- Gas Effect (13%): excessive gas content is locked in the pump, causing the current to drop rapidly because of the motor underload.

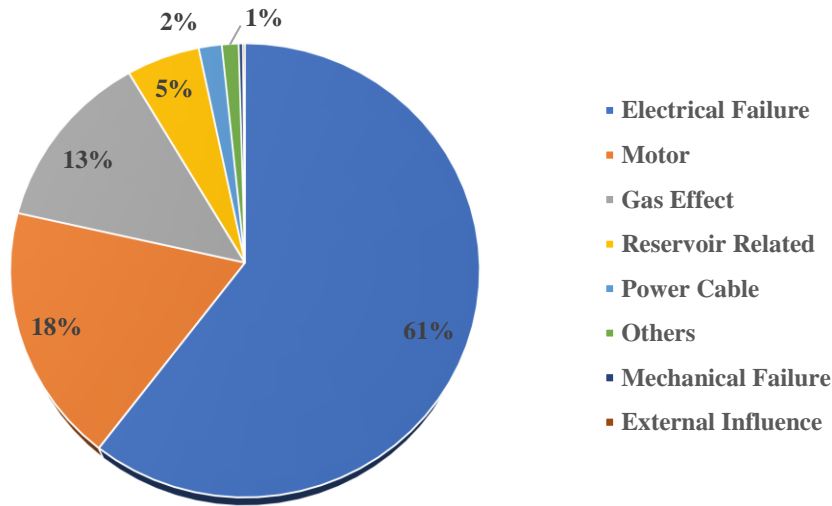


Figure 1 ESP Failure Statistical Analysis-General Descriptor.

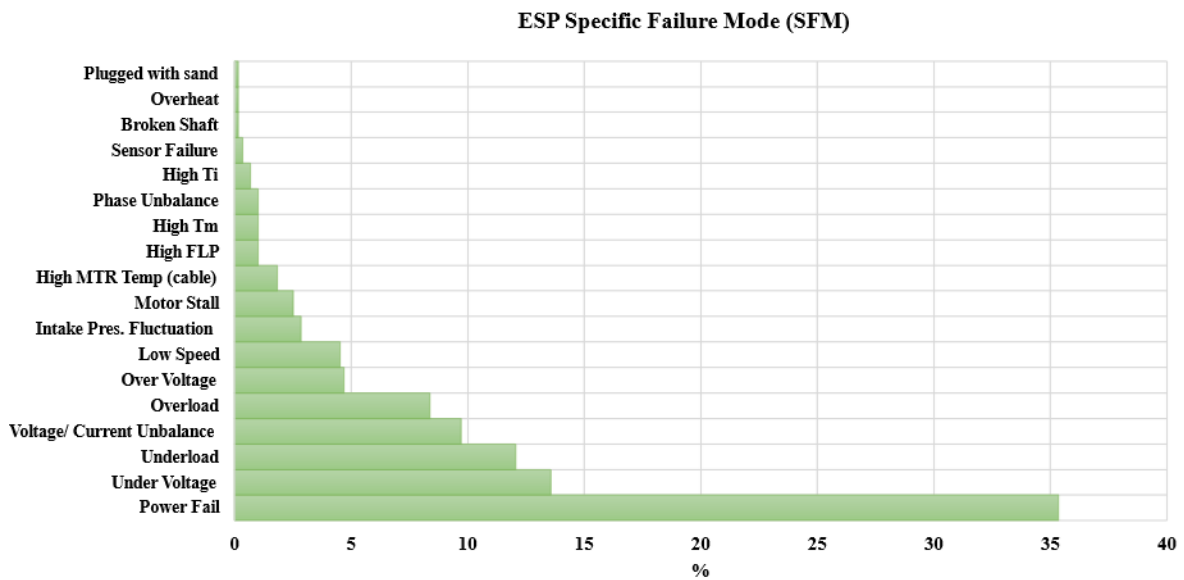


Figure 2 ESP Failure Statistical Analysis-Specific Failure Mode (SFM).

2.2 Case Studies

In this study, two specific cases will be presented in detail to discuss the types of failures and their corresponding effects on the ESP and the well’s production. The two most prevalent reasons shown above were observed in the cases analyzed. The ESP in Well #1 experienced an electrical failure, specifically phase unbalance. Well #2, on the other hand, experienced electrical failure induced by an overcurrent. Both cases share a common general reason for failure but have distinct underlying causes of failure. This highlights the need for recognizing and diagnosing the fundamental cause of ESP failure to choose the most effective course of action to mitigate it. Each case includes the failed ESP's history, the Dismantle Inspection, and Failure Analysis (DIFA) outcomes, and the underlying cause of failure.

2.2.1 Well #1

A downhole ESP pump is being used to produce oil from this vertical oil well with API gravity of 29°, average liquid production of 2,200 BPD, 76% water cut, and a gas-oil ratio (GOR) of 545 SCF/bbl. This ESP was installed and run in the well for 290 days (9 months). Figure 3 depicts the wellbore schematic for Well #1. The system suffered unstable intake pressure (Pi) and fluctuations in all running parameters (wellhead pressure, flowline pressure, Vibration, Amps, etc.). The downhole sensor readings were lost a week before the failure, and the system tripped on overload. The preliminary cause of failure for this ESP was diagnosed as electrical failure resulting in a burn in the Motor Lead Extension (MLE), as seen in Figure 4.

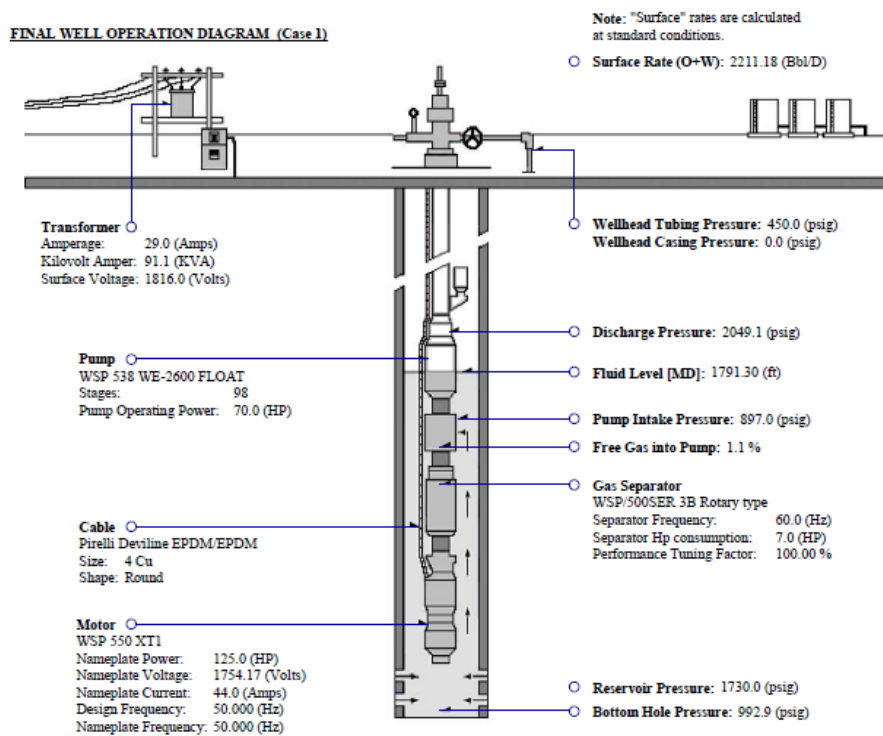


Figure 3 Well #1 Wellbore Schematic.

During the DIFA, the housing was dismantled, severe wear was found on all stages, a scale-like material on the outside of the diffuser, and emulsion/foamy fluid on the outside of the top 16 diffusers, and a hole on the diffuser due to severe wear. Regarding electronics, the MLE cable was blown out 24 ft above the pothead, and the main power cable had a thick layer of scale-like material. Apart from the MLE cable, the cable was verified to be electronically sound.

Many factors contributed to the wear of the pump's stages over its lifespan, including fluid type, scale/solids, backpressure, and down-thrust. The formation's scale-like material caused severe wear, resulting in power overload. Overload increased current draw, resulting in overheating and the cable blowing out. This wear caused a hole in the pump, and as a result, the MLE cable at the hole location was shorted. Table 2 summarizes the failure analysis results for Well #1 based on the DIFA report. The root cause of the failure in this situation was the well's Reservoir Performance.

Table 2 Well #1 Failure Analysis Clarifications.

Reason for Pull – General:	Electrical
Reason for Pull – Specific:	Phase Unbalance
Primary Failed Item:	ESP Cable
Secondary Failed Item:	Motor Lead Extension
General Failed Descriptor:	Electrical
Specific Failed Descriptor:	Short Circuit
General Failure Cause:	Reservoir or Fluids
Specific Failure Cause:	Reservoir Performance

A workover was performed to selectively re-perforate the formation based on Pulsed Neutron Capture (PNC) log results for water saturation and hydrocarbon layers. The well was then completed with a new ESP.

2.2.2 Well #2

A downhole ESP pump is being used to produce oil from a vertical oil well with API gravity of 30°, average liquid production of 3,000 BPD, 60% water cut, and a gas-oil ratio (GOR) of 428 SCF/bbl. This well was run with an ESP for 102 days (3 months). Figure 4 depicts the wellbore schematic for Well #2.

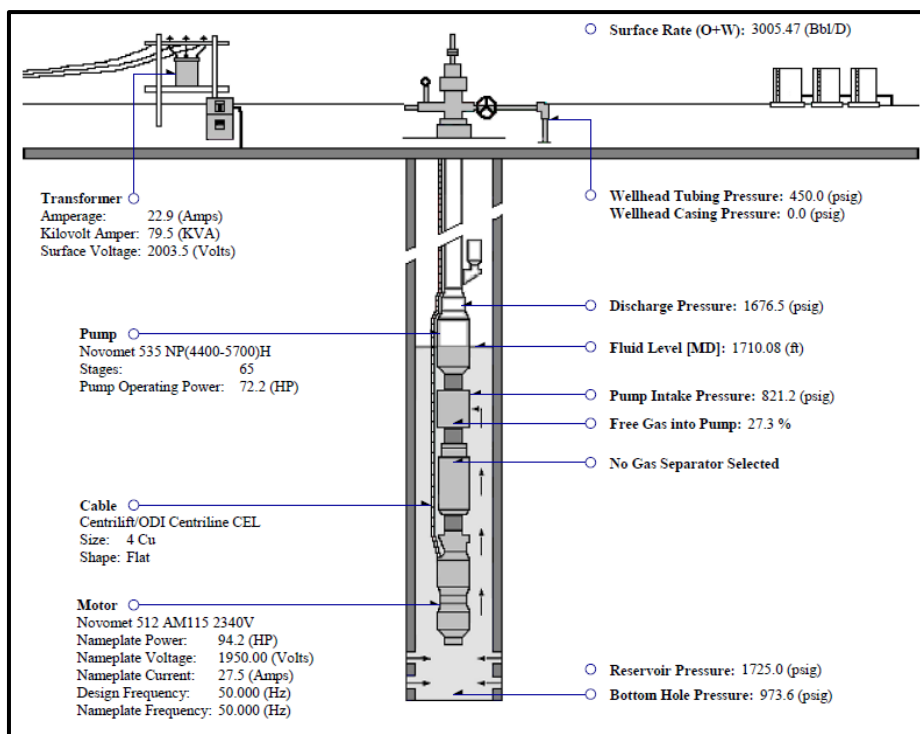


Figure 4 Well #2 Wellbore Schematic.

The well faced electrical failure due to overcurrent. The motor had two melted leads and was grounded. The cable suffered mechanical damage during the POOH, and its upper side had less

insulation resistance. The impellers and sleeves of the pump showed radial wear, with some fallback debris on the upper side. In addition, the pump stage washers had light upthrust wear.

Table 3 summarizes the Failure Analysis results for Well #2, based on the DIFA report. The most likely root cause of failure was filtered clogging with foreign material, resulting in reduced flow along the items inside the shroud and poor cooling. There was an overheat warning on the housing, indicating that the Motor had overheated, resulting in electronic failure. As a result, an upper sand trap was advised for installation.

Table 3 Well #2 Failure Analysis Clarifications.

Reason for Pull – General:	Electrical
Reason for Pull – Specific:	Overcurrent
Primary Failed Item:	ESP Motor
Secondary Failed Item:	Motor End Connectors (Y-point/Leads)
General Failed Descriptor:	Material
Specific Failed Descriptor:	Melted/Damaged
General Failure Cause:	Reservoir/Fluids
Specific Failure Cause:	Sand/Mud

2.3 ESP Specific Failures Overview

In this study, several distinct ESP failures are analyzed regarding the early warning signs before the actual failures. The trends in the data are depicted with time, starting from two weeks before each specific failure mode (SFM). Common warning signs are assessed using ten samples from each SFM presented in this section. The objective is to have a general understanding of the data trends associated with each SFM.

2.3.1 SFMs Associated with Electrical Failures

ESP electrical failures are prevalent and attributed to surface and downhole systems [14]. The downhole system fails if any of the electrical components in the ESP assembly fails, including the power cable, motor (i.e., stator), or downhole sensor. As shown earlier, electrical failures account for 61% of all ESP operational failures. The trends in the acquired data before some of the ESP electrical failures are shown in this section.

Under Voltage. The under-voltage specific failure is caused by the main power supply with inadequate control or a wiring problem. This SFM can cause the pump motor to overheat, resulting in motor failure. Multiple ESP variables are explored to identify the patterns before the actual failure. Figure 5 depicts motor voltage and current data for two weeks before under-voltage failures for two examples in Wells 2 and 4 of our datasets. The x-axis indicates the time before failure (TBF) in days. Both voltage and current diverge from their typical trends at almost the same time in both wells. The voltage of the motor in Well 2 begins to drop 0.8 days before failure and continues to decline until the actual failure. For Well 4, a reduction in voltage is first seen 2.1 days before failure, while the motor current increases. As the voltage of the motor drops, the motor draws greater current,

which causes the motor to overheat, resulting in sudden failure. These wells display early warning indicators of a condition requiring immediate attention.

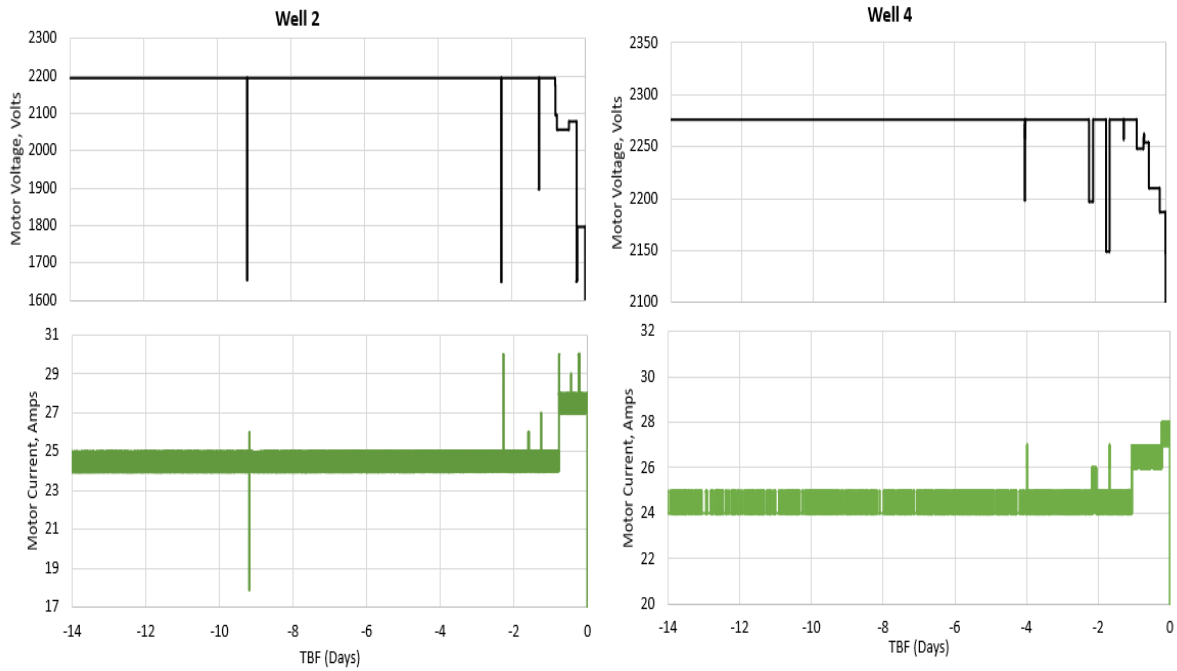


Figure 5 Under-voltage Specific Failure Effects on Motor Current and Voltage.

Power Fail. A power fail occurs due to unbalanced phases, voltage spikes, the presence of harmonics (distorted current and voltage), or lightning strikes. Consequently, the ESP motor and power cable are overheated. Takacs recommended a clean electric supply or a VSD unit with sinusoidal output to alleviate these issues [19].

Figure 6 depicts examples of motor voltage, motor current, and wellhead pressure for two weeks before two power failures in Wells 3 and 6. The figure shows the declining trend of wellhead pressure within a day before failure for both wells. In addition, voltage spikes (surges) are seen in Well 3 beginning 0.78 days before failure. Similar trends are found for the Well 6 case, where the spikes start 2.9 days before the failure. Voltage surge is the rapid increase in voltage over a very brief period in a power system [4]. In addition, the motor current in Well 3 exhibits an increasing trend three days before failure. A similar observation is made for Well 6, starting 2.8 days before the failure, showing early warning signs of a problem that demands attention.

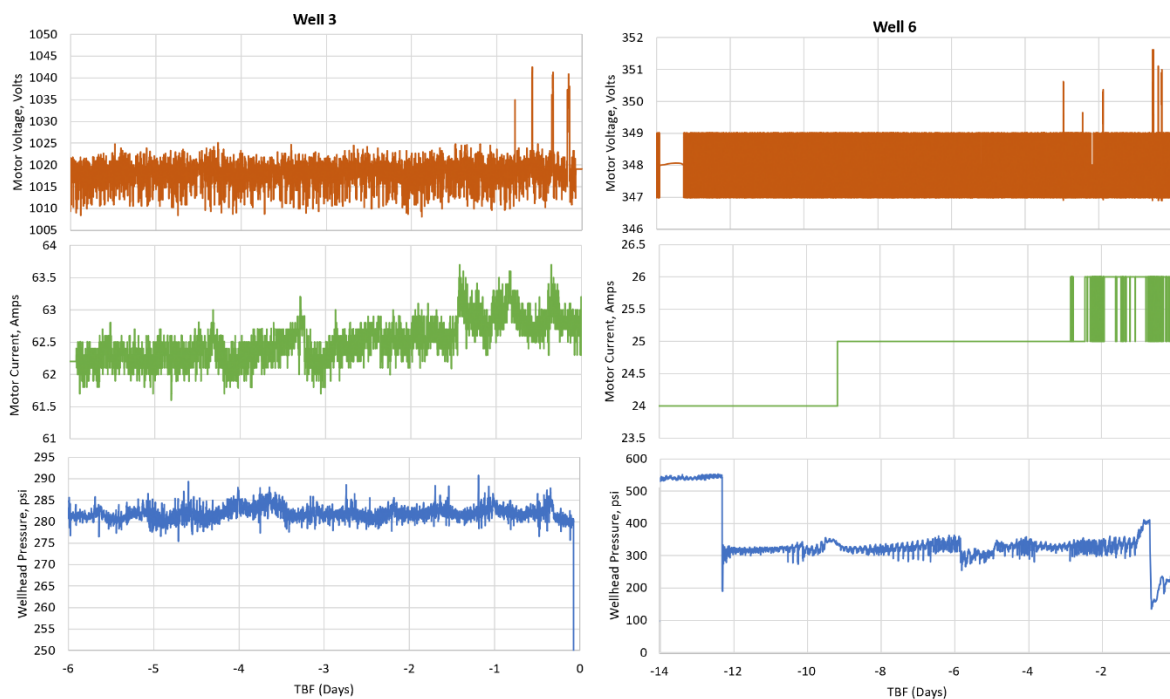


Figure 6 Power Fail Specific Failure Effects on Motor Voltage, Current, and Wellhead Pressure.

2.3.2 SFMs Associated with Motor Failures

Most ESP motor failures are due to electrical issues [14]. Based on the investigated field data, motor overload and high motor winding temperature are some motor-related failures. As shown earlier, motor failures account for 18% of all ESP operational failures. The trends in the acquired data before some of the ESP motor failures are shown in this section.

Motor Overload. An overload failure happens when the motor draws excessive current, resulting in excessive power consumption. As a result, the motor may overheat, leading to motor damage [14]. Various factors may contribute to an overload, including an improperly sized motor, an unexpectedly high fluid specific gravity raising the Total Dynamic Head (TDH) over the design value, and inconsistent motor voltage [15]. Figure 7 depicts wellhead pressure, motor current, and motor temperature trends for the two weeks before two cases of overload failures in Wells 3 and 10. The x-axis indicates the time before failure (TBF) in days. The figure shows the declining trend of wellhead pressure as failure time approaches for both wells. Moreover, the motor current in Well 3 suddenly increases three days before failure. The trend is similar for Well 10, where the deviation begins 1.8 days before the failure. The motor temperature also rises as the failure approaches, beginning 2.7 days in advance for Well 10 and 2.1 days before for Well 3. These wells may exhibit early warning signs of a problem that demands attention.

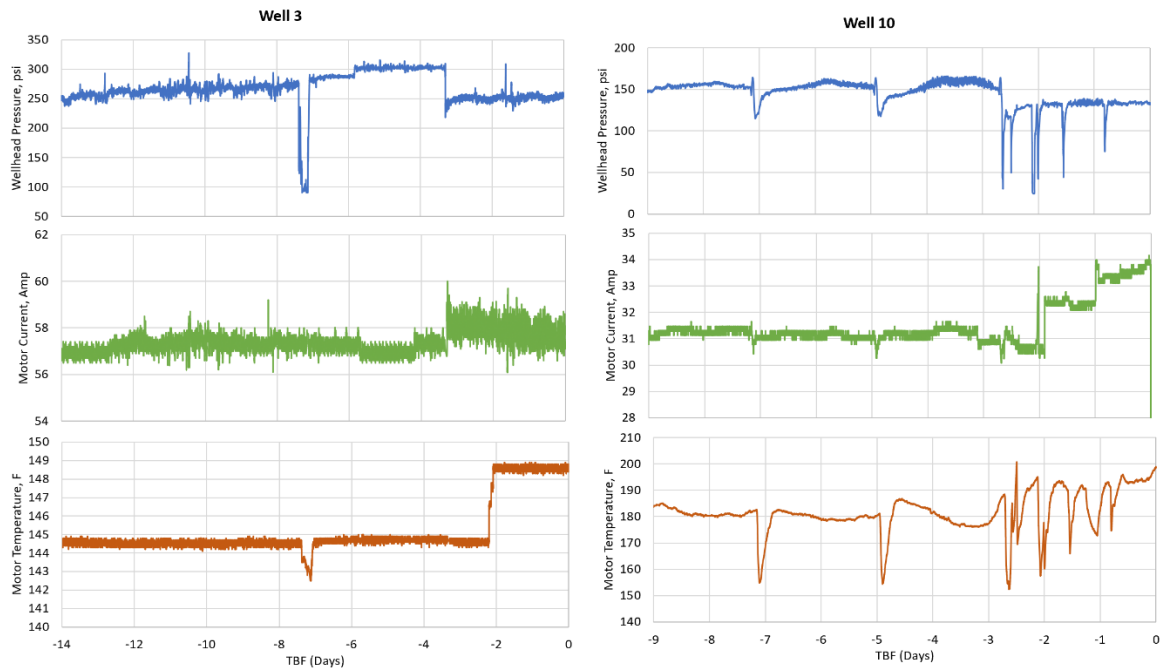


Figure 7 Motor Overload Specific Failure.

High Motor Temperature. A high motor temperature happens when excessive voltage supply or drawn motor current leads to overheating issues [4]. Overheating is a primary cause of motor failure, particularly when the motor is forced to work harder or is placed under an unexpected load. As the speed of the motor and, by extension, the rotation of the pump's shaft rises, the moving components get overheated due to the increased friction [29]. Figure 8 displays motor voltage, current, and temperature before two cases of motor temperature failure in Wells 8 and 1. The x-axis represents the TBF in days. The graph depicts the increasing trend of motor current as the failure time for both wells' approaches. In addition, the motor voltage in Well 8 surges rapidly 0.6 days before the failure. A similar observation is made for Well 1, where the deviation starts one day before the failure. As the failure nears, the motor temperature increases, starting 0.8 days before failures in both wells. These wells display early warning signals of a serious situation.

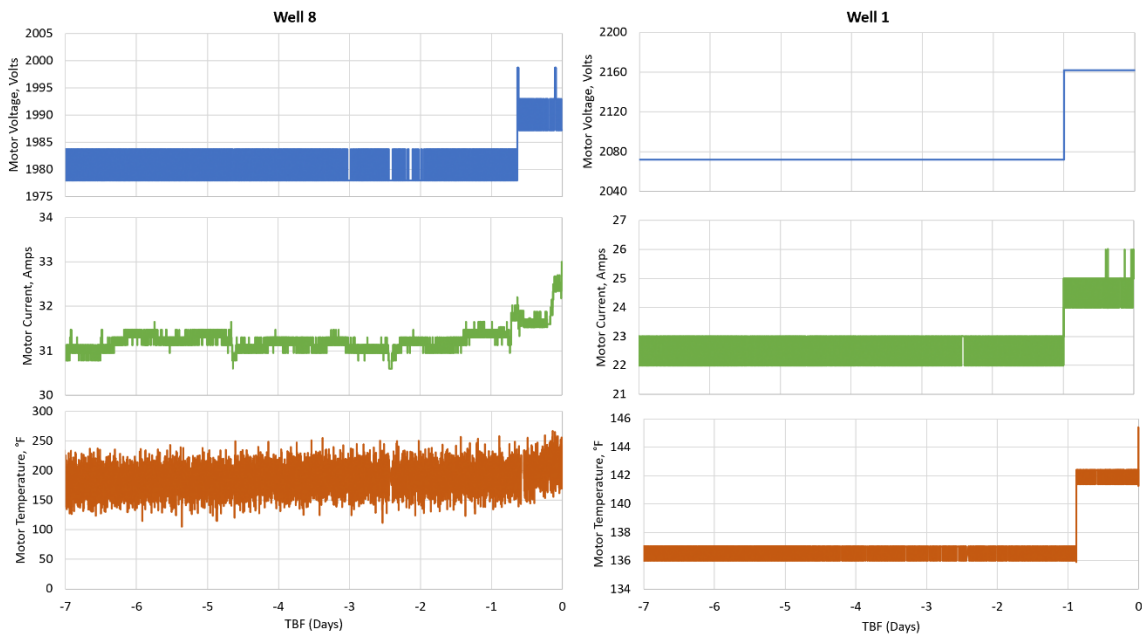


Figure 8 High Motor Temperature Specific Failure.

2.3.3 SFMs Associated with Other Failures

Motor Underload. An underload failure often indicates pumped-off or gas-locked conditions [19]. Different high-frequency ESP variables were investigated to observe the patterns before the failure. Figure 9 depicts pump intake pressure and motor current during the two weeks before two examples of underload failures in Well 8 and Well 9. The x-axis indicates the time before failure (TBF). The figure shows the rising trend of pump intake pressure as failure time approaches for both wells. Moreover, the motor current in Well 8 deviates from its regular pattern at 6.3 days, with a decreasing trend as the failure approaches. A similar observation is made for Well 9, where the deviation begins 1.8 days before the failure.

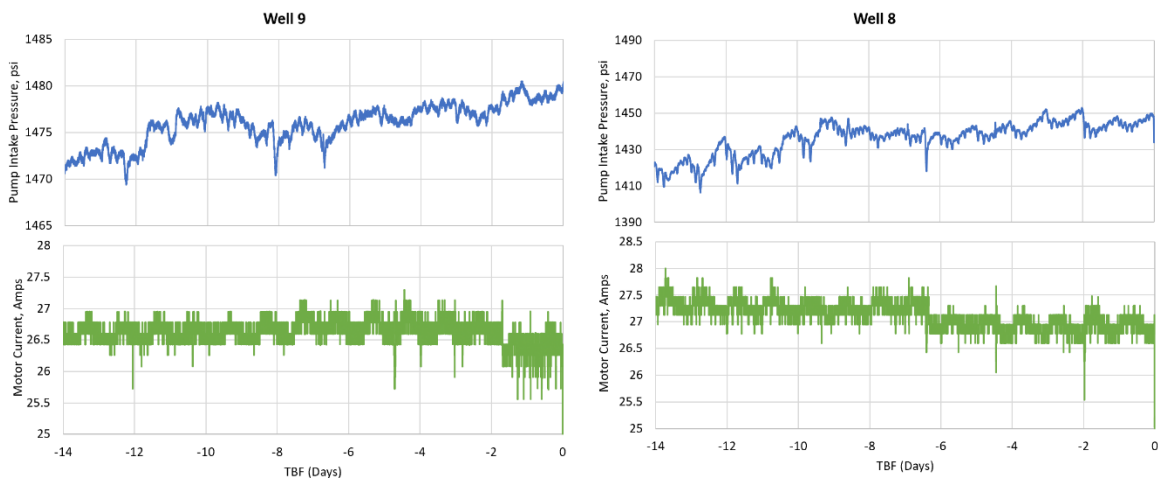


Figure 9 Underload Failure Prior Data Trends.

2.4 Summary

Table 4 summarizes the described specific ESP failure modes with their early warning signs in the ESP parameters. The average time before the failure (TBF), when each sign starts to appear, is also included based on the ESP failure data of this study. These qualitative observations can be used as a general guideline to identify the ESP operational issues earlier and with less effort.

Table 4 Each ESP SFM with its Early Warning Signs, Based on the Data of This Study.

SFM	Early Signs	Average TBF (Days)
High Motor Temperature	Motor current increases	1.1
	Motor voltage increase	1.7
	Motor temperature increases	0.8
High Cable Temperature	Motor voltage increases	1.1
	Motor current increase	1
Overload	Wellhead pressure drops	3.1
	Motor current increase	2.4
	Motor temperature increase	2.4
Plugged with sand	Hard start followed by motor current spikes	2.5
	Voltage spikes	1.85
Power Fail	Current increases	2.9
	Wellhead pressure drops	0.7
Sensor Failure	Motor Voltage spikes and continue increasing	1.5
Under Voltage	Motor voltage drops	3.7
	Motor current Increases	1.4
Underload	Pump intake pressure increases	2.5
	Motor current decreases	3.9

3. ESP Reliability Analysis

This section discusses the reliability analysis of ESP failures, where the probability of ESP failure is a key metric. Reliability analysis is an extensively studied statistical technique for forecasting systems' performance in various sectors [30]. It denotes the probability of fully functioning during a specific time interval [30]. Mean Time Between Failures (MTBF) is strongly associated with this concept, with a longer MTBF indicating greater system reliability [31]. Accurate evaluation and forecasting of ESP failure probability contribute to a deeper comprehension of system performance. Mean time between failures (MTBF) quantifies the average time it takes for a system to fail. MTBF measurements may be used to evaluate ESP performance, design, and reliability. MTBF is defined as the arithmetic mean value of the reliability function, $R(t)$, which is the predicted value of the time till failure density function, $f(t)$ [31].

$$MTBF = \int_0^{\infty} R(t)dt = \int_0^{\infty} t f(t) dt \tag{1}$$

$$f(t) = \lambda e^{-\lambda t} \tag{2}$$

where λ is the failure rate.

For the case of this study, Equation 3 may be used to calculate the MTBF. In addition, Equation 4 may be used to calculate the failure rate.

$$MTBF = \frac{\sum(\text{Start of Downtime of Current Failure} - \text{Start of Uptime after last Failure})}{\text{Number of failures}} \quad 3$$

$$\text{FailureRate} = \frac{1}{MTBF} * 100 \quad 4$$

The ESP’s MTBF trend for the 10 wells over the five years is shown in Figure 10. Initially, all wells had a maximum MTBF of 46 to 354 days. The MTBF decreases with time, particularly in the third year of operation (2019), until it reached its lowest value in 2021. In 2017, Well 1 had the longest MTBF of 354.5 days, while the lowest was 46 days for Well 6. After five years, in 2021, Well 8 had the longest MTBF of 38 days, while Well 3 had the shortest duration of 10.9 days. The failure rates of ESPs in the ten wells can also be calculated using Equation 4 throughout the five-year production period. The failure rates of Well 6 and Well 7 are consistently more significant than those of the other wells.

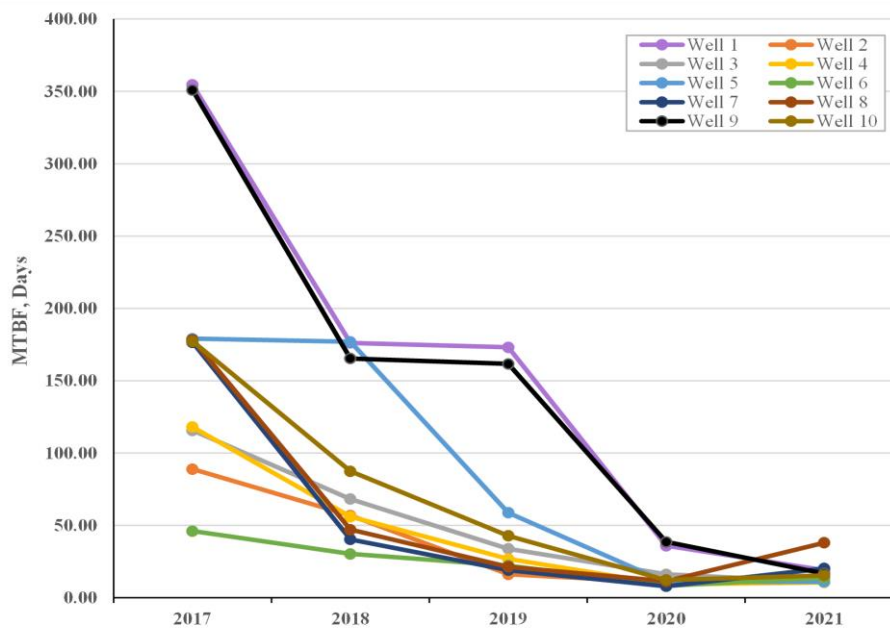


Figure 10 ESP’s MTBF for all wells over five years of production.

Now let’s focus on wells 6 and 7, as the wells with the highest failure rates. Figure 11 shows the specific failure modes by subcategory for these wells. For Well 6, power failure accounts for 71% of all SFMs, while the remaining 29% is almost evenly split across MTR cable, overload, under voltage, and underload. For Well 7, power failure accounts for 72% of all SFMs, while overload is 15%, Undervoltage is 9%, and overvoltage is 4%.

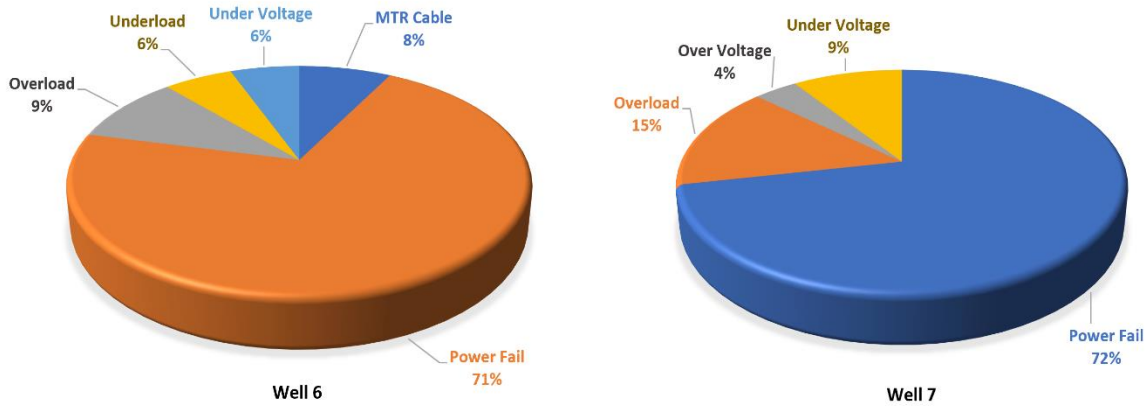


Figure 11 ESP's Specific Failure Mode (SFM) for Well 6 and Well 7.

3.1 Weibull Analysis

Failure data can be modelled using various distributions, including normal, exponential, Rayleigh, Weibull, gamma, and lognormal. Weibull Analysis is an efficient statistical data analysis technique for assessing time dependence. The two-parameter Weibull distribution is defined as follows [15]:

$$f(t) = \frac{\beta}{\eta} \left(\frac{t}{\eta}\right)^{\beta-1} e^{-\left(\frac{t}{\eta}\right)^\beta} \quad 5$$

where β is the shape parameter, η is the scale parameter, and t represents the value to be evaluated.

The shape factor (β) determines the distribution's behavior. The failure rate drops with time if $\beta < 1$, meaning that the ESP gets more trustworthy as it matures. Manufacturing or installation errors may be a cause of this. The failure rate increases if $\beta > 1$, mainly due to pump wear. Finally, if $\beta = 1$, it denotes a consistent failure rate that is time independent.

Based on the field data from 10 wells, a Weibull model is built to estimate the probability of failure. The previously estimated MTBF values are utilized as inputs to the Weibull analysis model. Next, the Weibull shape and scale parameters are estimated using Median Rank Regression. Then the Weibull Probability plots are generated. On logarithmic scales, these plots depict unreliability, defined as the probability of failure (%) vs. time to failure (days).

Figure 12 illustrates Well 6's and Well 7's unreliability plots, respectively. The legend indicates the number of MTBF points (5 points for five years), Weibull parameter estimates (β and η), confidence limits used (Beta-Binomial Bounds), and the degree of confidence (90%). The Weibull line accurately fits the MTBF points in both plots with R^2 values of 99.4% and 86.5%, respectively, and a low p-value. The predicted Weibull parameters for Well 6 are β of 1.538 and η of 28. A $\beta > 1$ value is a sign of pump wear and increasing failure rate with time. According to the plot, the ESP in Well 6 has a 90% probability of failure after 75 days of the previous failure. The probability of failure increases to 99% in 80 days.

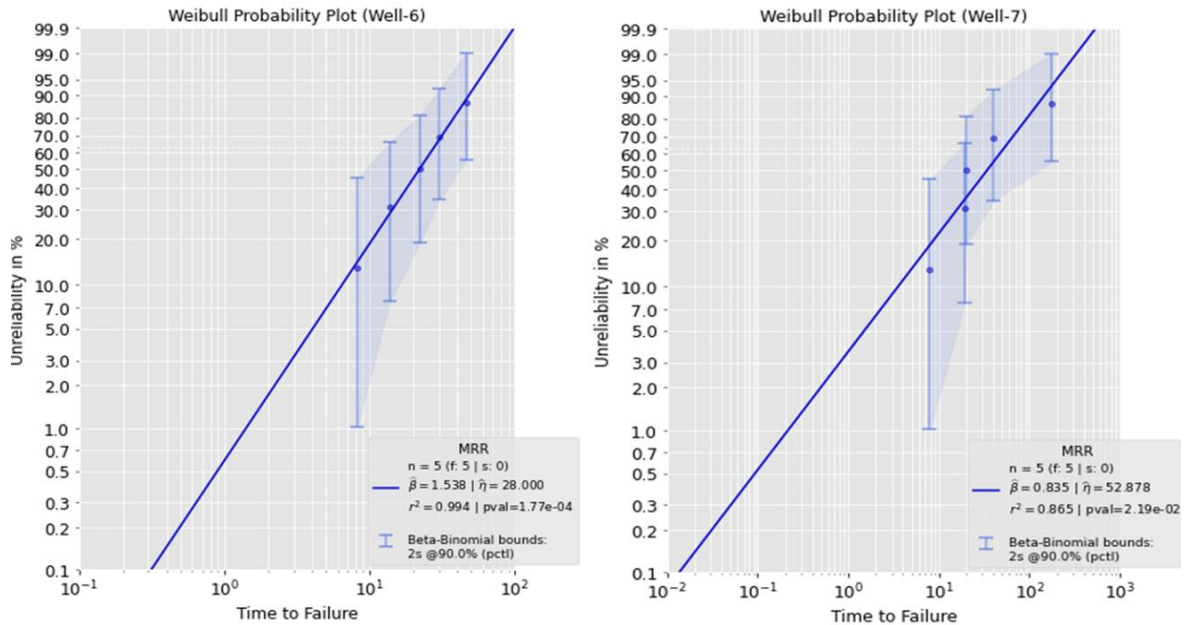


Figure 12 Weibull Analysis for Failure Probabilities of Well 6 and Well 7.

From Figure 12, the predicted Weibull parameters for Well 7 are β of 0.835 and η of 52.87, a possible indicator of manufacturer errors in the early life of the well. According to the plot, the ESP has a 90% probability of failure after 190 days. The predicted failure probability increases to 99% in 300 days. Comparing both ESP wells, well 7 is more reliable than well 6, as the 90 percent probability of failure occurs after 190 days vs. 75 days in well 6.

4. Conclusions

This study analyzes the field data collected from surface and downhole ESP monitoring equipment of 10 wells over a 5-year production period. According to these data, three common categories of ESP failures are electrical failures (61%), motor failures (18%), and gas effects (13%). Looking more specifically, power failure, under-voltage, voltage unbalance, and motor underload are the most common occurrences. Two field case studies from two wells in Kuwait Oil Company (KOC) assets are discussed in depth to explore the failure types and their related consequences on the ESP and the well's production. These cases of electrical failure have distinct underlying causes of phase unbalance and overcurrent, respectively. Diagnosing the root cause of ESP failure is essential for identifying the best line of action to mitigate it.

The early warning signs of failures are investigated by looking at the data trends within the two weeks before each SFM. On average, the warning signals of ESP failure manifest themselves two days before the failure, depending on the SFM. The most impacted variables are the motor current and voltage, consistent with the fact that most ESP failures are electrical for the data under investigation.

The Weibull statistical analysis is used to assess the ESP reliability, predicting the probability of ESP failure and the MTBF values. The ESP's MTBF trends for the ten wells are estimated over five years. Initially, all wells had long MTBF values (higher reliability). The MTBF drops with time, starting from the third year of operation. Consequently, ESP loses its reliability over time as operational

issues cause an increasing number of failures. This model aids in the forecasting of ESP failure probability.

Author Contributions

Conceptualization: H Karami and D Devegowda; Field data acquisition and literature review: S. AlBallam and H Karami; Reliability analysis: S Alballam; Supervision: H Karami and D Devegowda. All authors have read and agreed to the published version of the manuscript.

Competing Interests

All Authors wish to confirm that there are no known conflicts of interest associated with this publication, and there has been no significant financial support for this work that could have influenced its outcome.

Additional Materials

The following additional materials are uploaded at the page of this paper.

1. Table S1: The Likely Specific Causes of Electrical Failures.
2. Table S2: The Likely Specific Causes of Motor Failures.
3. Table S3: The Likely Specific Causes of Gas Effect Failure.
4. Table S4: The Descriptions of the Other ESP Specific Failures.

References

1. Igwilo KC, Okoro EE, Ubanatu S. Comparative approach to optimum selection of artificial lift system. *Pet Coal*. 2018; 60: 429-437.
2. Nguyen T. Artificial lift selection methodology for vertical and horizontal wells in conventional and unconventional reservoirs. In: *Artificial lift methods: Design, practices, and applications*. Cham: Springer; 2020. pp. 317-347.
3. Fakher S, Khlaifat A, Hossain ME, Nameer H. Rigorous review of electrical submersible pump failure mechanisms and their mitigation measures. *J Petrol Explor Prod Technol*. 2021; 11: 3799-3814.
4. Takacs G. *Electrical submersible pumps manual: Design, operations, and maintenance*. Netherlands: Elsevier Science; 2009.
5. El Gindy M, Abdelmotaal H, Botros K, Ginawi I, Sayed E, Edris T. Monitoring & Surveillance improve ESP operation and reduce workover frequency. *Proceedings of Abu Dhabi International Petroleum Exhibition and Conference*; 2015 November 9-12; Abu Dhabi, UAE. Richardson, Texas: OnePetro. doi: 10.2118/177926-MS.
6. Abdelaziz M, Lastra R, Xiao JJ. ESP data analytics: Predicting failures for improved production performance. *Proceedings of Abu Dhabi International Petroleum Exhibition & Conference*; 2017 November 13-16; Abu Dhabi, UAE. Richardson, Texas: OnePetro. doi: 10.2118/188513-MS.
7. Mohrbacher JD. A field study of ESP performance in a deep, hot, and sour environment. *Proceedings of SPE Rocky Mountain Regional Meeting*; 1984 May 21-23; Casper, Wyoming, USA. Richardson, Texas: OnePetro. doi: 10.2118/12913-MS.

8. Tabe FL. An overview of the installation, operation, maintenance, and problems associated with electrical submersible pump system in central Sumatra, Indonesia. Proceedings of SPE Annual Technical Conference and Exhibition; 1984 September 16-19; Houston, Texas, United States. Richardson, Texas: OnePetro. doi: 10.2118/13201-MS.
9. Higgs G. ESP performance – A statistical review. Proceedings of 3rd European Electrical Submersible Pump Round Table; 1994; Aberdeen, Scotland, United Kingdom. BP Exploration.
10. Venkataraman G, Mikus T. Reliability analysis of electrical submersible pumps. Proceedings of 1994 SPE ESP Workshop; 1994; Houston, Texas, USA. Shell Development Company.
11. Oliveira LF, Bardy MB, Filho SS, Neves EA, Silva JA, Agustoni JA, et al. Analysis of ESP failure data from the northeastern pole of the Campos oil basin. Proceedings of ESP Workshop; 1997 April 30-May 2; Houston, Texas, USA.
12. Patterson MM. A model for estimating the life of electrical submersible pumps. SPE Prod Fac. 1993; 8: 247-250.
13. Sawaryn SJ, Norrell KS, Whelehan OP. The analysis and prediction of electric-submersible-pump failures in the Milne point field, Alaska. Proceedings of SPE Annual Technical Conference and Exhibition; 1999 October 3-6; Houston, Texas, USA. Richardson, Texas: OnePetro. doi: 10.2118/56663-MS.
14. Alhanati FJS, Solanki SC, Zahacy TA. ESP failures: Can we talk the same language? Proceedings of SPE Gulf Coast Section Electric Submersible Pump Workshop; 2001 April 25-27; Houston, Texas, USA. Richardson, Texas: OnePetro. doi: 10.2118/148333-MS.
15. Sawaryn SJ, Grames KN, Whelehan OP. The analysis and prediction of electric submersible pump failures in the Milne point field, Alaska. SPE Prod Fac. 2002; 17: 53-61.
16. Sawaryn SJ, Ziegel E. Statistical assessment and management of uncertainty in the number of electric-submersible pump failures in a field. Proceedings of SPE Annual Technical Conference and Exhibition; 2001 September 30-October 3; New Orleans, Louisiana, USA. Richardson, Texas: OnePetro. doi: 10.2118/71551-MS.
17. Sawaryn SJ. The dynamics of electrical-submersible-pump populations and the implication for dual-ESP systems. SPE Prod Fac. 2003; 18: 236-246.
18. Liu Y, Yao K, Liu S, Raghavendra CS, Lenz TL, Olabinjo L, et al. Failure prediction for rod pump artificial lift systems. Proceedings of SPE Western Regional Meeting; 2010 May 27-29; Anaheim, California, USA. Richardson, Texas: OnePetro. doi: 10.2118/133545-MS.
19. Takacs G. Electrical submersible pumps manual: Design, operations, and maintenance. Gulf professional publishing; 2017.
20. Williams AJ, Cudmore J, Beattie S. ESP monitoring – Where's your speedometer? Proceedings of 7th European Electric Submersible Pump Round Table, Aberdeen Section Table; 2003 April 30-May 2; Houston, Texas, USA.
21. Sherif S, Adenike O, Obehi E, Funso A, Eyituyo B. Predictive data analytics for effective electric submersible pump management. Proceedings of SPE Nigeria Annual International Conference and Exhibition; 2019 August 5-7; Lagos, Nigeria. Richardson, Texas: OnePetro. doi: 10.2118/198759-MS.
22. Gupta S, Nikolaou M, Saputelli L, Bravo C. ESP health monitoring KPI: A real-time predictive analytics application. Proceedings of SPE Intelligent Energy International Conference and Exhibition; 2016 September 6-8; Aberdeen, Scotland, UK. Richardson, Texas: OnePetro. doi: 10.2118/181009-MS.

23. Adesanwo M, Denney T, Lazarus S, Bello O. Prescriptive-based decision support system for online real-time electrical submersible pump operations management. Proceedings of SPE Intelligent Energy International Conference and Exhibition; 2016 September 6-8; Aberdeen, Scotland, UK. Richardson, Texas: OnePetro. doi: 10.2118/181013-MS.
24. Bermudez F, Carvajal GA, Moricca G, Dhar J, Md Adam F, Al-Jasmi A, et al. Fuzzy logic application to monitor and predict unexpected behavior in electric submersible pumps (part of the KwIDF project). Proceedings of SPE Intelligent Energy Conference & Exhibition; 2014 April 1-3; Utrecht, The Netherlands. Richardson, Texas: OnePetro. doi: 10.2118/167820-MS.
25. Grassian D, Bahatem M, Scott T, Olsen D. Application of a fuzzy expert system to analyze and anticipate ESP failure modes. Proceedings of Abu Dhabi International Petroleum Exhibition & Conference; 2017 November 13-16; Abu Dhabi, UAE. Richardson, Texas: OnePetro. doi: 10.2118/188305-MS.
26. Pennel M, Hsiung J, Putcha VB. Detecting failures and optimizing performance in artificial lift using machine learning models. Proceedings of SPE Western Regional Meeting; 2018 April 22-26. Garden Grove, California, USA. Richardson, Texas: OnePetro. doi: 10.2118/190090-MS.
27. Mubarak HA, Khan FA, Oskay MM. ESP failures / analysis / solutions in divided zone – case study. Proceedings of Middle East Oil Show; 2003 June 9-12; Bahrain. Richardson, Texas: OnePetro. doi: 10.2118/81488-MS.
28. Al-Sadah H. ESP data analysis to enhance electrical submersible pump run life at Saudi Arabian fields. Proceedings of SPE Middle East Artificial Lift Conference and Exhibition; 2014 November 26-27; Manama, Bahrain. Richardson, Texas: OnePetro. doi: 10.2118/173703-MS.
29. Betonico GC, Bannwart AC, Ganzarolli MM. Determination of the temperature distribution of ESP motors under variable conditions of flow rate and loading. J Pet Sci Eng. 2015; 129: 110-120.
30. Lastra R. The quest for the ultrareliable ESP. Proceedings of SPE Middle East Artificial Lift Conference and Exhibition; 2016 November 30-December 1; Manama, Kingdom of Bahrain. Richardson, Texas: OnePetro. doi: 10.2118/184169-MS.
31. Birolini A. Reliability engineering: Theory and practice. Springer Science & Business Media; 2013.



Enjoy *JEPT* by:

1. [Submitting a manuscript](#)
2. [Joining in volunteer reviewer bank](#)
3. [Joining Editorial Board](#)
4. [Guest editing a special issue](#)

For more details, please visit:

<http://www.lidsen.com/journal/jept>